Published in final edited form as:
J Immunol. 2013 September 1; 191(5): 2184–2193. doi:10.4049/jimmunol.1301221.

Complement activation associated with ADAMTS13 deficiency in human and murine thrombotic microangiopathy

Ramesh Tati[*], **Ann-Charlotte Kristoffersson**[*], **Anne-lie Ståhl**[*], **Johan Rebetz**[*], **Li Wang**[§], **Christoph Licht**[¶], **David Motto**[§], and **Diana Karpman**[*]

[*]Department of Pediatrics, Clinical Sciences Lund, Lund University, Lund, Sweden

[§]Department of Internal Medicine and Pediatrics, University of Iowa College of Medicine, Iowa City, IA

[¶]Division of Nephrology, The Hospital for Sick Children and University of Toronto, Toronto, Canada

Abstract

This study addressed the contribution of ADAMTS13-deficiency to complement activation in thrombotic thrombocytopenic purpura (TTP). Renal tissue and blood samples were available from 12 TTP patients. C3 and C5b-9 deposition were demonstrated in the renal cortex of two TTP patients, by immunofluorescence and immunohistochemistry, respectively. C3 was also demonstrated in the glomeruli of Shiga toxin-2 treated *Adamts13*$^{-/-}$ mice (n=6 of 7) but less in mice that were not Shiga toxin-2-treated (n=1 of 8, $p<0.05$) or wild-type mice (n=0 of 7). TTP patient plasma (n=9) contained significantly higher levels of complement-coated endothelial microparticles than control plasma (n=13), as detected by flow cytometry. Exposure of histamine-stimulated primary glomerular endothelial cells to platelet-rich-plasma from patients, or patient platelet-poor-plasma combined with normal platelets, in a perfusion system, under shear, induced C3 deposition on von Willebrand factor (VWF)-platelet strings (on both VWF and platelets) and on endothelial cells. Complement activation occurred via the alternative pathway. No C3 was detected when cells were exposed to TTP plasma that was pre-incubated with EDTA or heat-inactivated, or to control plasma. In the perfusion system patient plasma induced more release of C3- and C9-coated endothelial microparticles compared to control plasma. The results indicate that the microvascular process induced by ADAMTS13 deficiency triggers complement activation on platelets and the endothelium, which may contribute to formation of thrombotic microangiopathy.

Introduction

Thrombotic microangiopathy (TMA) is a pathologic lesion occurring at the interface of the endothelium and the bloodstream in which the endothelium is injured and intraluminal thrombosis ensues, followed by obstruction of the vessel (1). The major forms of TMA are thrombotic thrombocytopenic purpura (TTP) and hemolytic uremic syndrome (HUS). TTP is associated with deficient levels or function of ADAMTS13, the von Willebrand factor (VWF)-cleaving protease (2). TTP may be congenital (3), due to mutations in ADAMTS13

Corresponding author: Diana Karpman, Department of Pediatrics, Lund University, 22185 Lund, Sweden Telephone number: +46 46 2220747, Fax number: +46-46-2220748 Diana.Karpman@med.lu.se.

Disclosures

Dr Licht has received unrestricted grants and fees from Alexion Pharmaceuticals for consultancy and invited talks as well as fees from CSL Behring for consultancy and invited talks. Dr Karpman was the national coordinator in Sweden of the international trial of Eculizumab (Alexion) during 2009-2010. The other authors declare no competing financial interests.

(Upshaw-Schulman syndrome), or acquired (4), associated with anti-ADAMT13 antibodies. HUS may be subdivided based on etiology in which the major subtypes are Shiga toxin (Stx)-associated or atypical complement-mediated HUS (5).

The kidney is affected in TTP and HUS with typical TMA lesions. Endothelial injury and platelet activation may be primary or secondary events in TMA. In HUS the endothelium and platelets are directly activated by bacterial toxin or complement deposition (6-10) whereas in TTP endothelial and platelet involvement occur secondary to the release of ultra-large VWF (ULVWF) multimers with high biological potency to bind platelets and form ULVWF-platelet aggregates leading to thrombosis (11).

Complement activation may contribute to formation of the TMA lesion, as shown in HUS. Stx induced P-selectin-mediated complement deposition on microvascular endothelial cells resulting in thrombus formation (9). Wild-type mice injected with Stx and lipopolysaccharide exhibited glomerular fibrinogen deposition whereas factor B-deficient mice were protected, indicating a role for the alternative pathway of complement in this model. Likewise, Stx bound to and activated platelets leading to complement deposition and activation via the alternative pathway (7). Stx was thus demonstrated to induce complement activation and thrombus formation both on the endothelium and on platelets. In atypical HUS complement activation occurs due to mutations in complement factors or regulators resulting in injury to endothelial cells (10, 12) and platelet activation (13), thereby initiating a pro-thrombotic process. Thus complement activation may play a role in enhancing endothelial injury and platelet activation occurring during TMA.

In TTP dysfunctional proteolysis of ULVWF allows an intravascular pro-thrombotic process to occur. Patients may have repeated episodes of TTP as well as symptom-free periods. Triggering events may induce thrombosis by initiating endothelial cell injury. This phenomenon was demonstrated in ADAMTS13-deficient mice that were basically symptom-free when on a non-susceptible genetic background (*Adamts13*$^{B/129-/-}$). Introduction of the CASA/Rk genetic background resulted in TTP susceptibility in which mice developed a severe TTP-like syndrome when endothelial cell injury was induced by challenge with Stx (14).

TTP patients were found to have elevated C3a and sC5b-9 during acute episodes (15). Serum from patients with ADAMTS13 deficiency induced C3 deposition and membrane-attack-complex formation on microvascular endothelial cells (16). The aim of this study was to demonstrate complement activation in renal tissue (human TTP, or murine after challenge with Stx2) and on circulating endothelial microparticles in TTP, and to study how ADAMTS13 deficiency promotes complement activation on the glomerular endothelium and endothelial microparticles as well as on VWF-platelet strings.

Materials and methods

Patients and controls

Nine patients with congenital TTP and 3 patients with acquired TTP were included in the study (Table I). All patients had renal involvement during acute episodes and all had ADAMTS13 activity < 5%. Some of these patients and their mutations have been previously described (17-22). Renal tissues were available from Patients 1-2 and blood samples (taken during remission) were available from Patients 3-12.

Control renal tissue was available from a nephrectomized kidney removed from an adult male with renal cancer from which tissue was taken from an unaffected area (22). Blood samples were available from 22 healthy adult volunteers (8 male, 14 female) not using any

medications. The study was conducted with the approval of the Ethics Committee of the Medical Faculty of Lund University and with the written informed consent of all patients, or their parents if younger than 15 years old, and controls.

Blood samples

Whole blood from patients and controls was drawn by venipuncture into vacutainer tubes (Becton Dickinson, Franklin Lakes, NJ) containing 0.5 mL of 0.129M or 0.27 ml of 0.109M sodium citrate, platelet-rich-plasma (PRP), platelet-poor-plasma (PPP) and washed platelets were obtained as previously described (13). Serum was obtained from blood drawn into BD vacutainer serum tubes (Becton Dickinson) as described (13). PRP was used within 4 hours of sampling. PPP and sera were stored in aliquots at −80°C until used. To prevent polymerization of fibrin Gly-Pro-Arg-Pro (GPRP, 10μM, Sigma-Aldrich, St. Louis, MO) was added to plasma samples before usage (6). At the start of some experiments, serum or plasma samples were diluted 1:1 with Dulbecco's phosphate buffered saline (DPBS, PAA Laboratories, Gmbh, Pasching, Austria) with or without Ca^{+2} and Mg^{+2}.

Mice

All animal studies were carried out with the approval of the University of Iowa Institutional Animal Care and Use Committee. Renal tissues were collected from ADAMTS13-deficient *Adamts13*$^{-/-}$ (n=11), heterozygous *Adamts13*$^{+/-}$ (n=7) and wild-type *Adamts13*$^{+/+}$ mice (n=4). Mice were available on two genetic backgrounds: *Adamts13B/CN1*$^{-/-}$ n=1 and *Adamts13B/CN1*$^{+/+}$ n=1 (mixed B/129, C57BL/6 and CASA/Rk genetic background) (14) and *Adamts13*$^{-/-}$ n=10, *Adamts13*$^{+/-}$ n=7 and *Adamts13*$^{+/+}$ n=3 (mixed C57BL/6 and CAST/Ei genetic background) (23).

Stx2 was injected in order to induce endothelial cell injury and a TTP-like phenotype (14). Mice were injected with Stx2 (250 pg/g, Sigma-Aldrich) or phosphate buffer saline (PBS, 10 μl/g, Invitrogen, Carlsbad, CA) via the lateral tail vein and subsequently sacrificed as indicated. Complete blood count analysis was performed on each mouse prior to sacrifice as described previously (23).

A preliminary experiment was carried out in the two mice with the *Adamts13 B/CN1* background. Mice were sacrificed three (*Adamts13 B/CN1*$^{-/-}$) or 10 (*Adamts13 B/CN1*$^{+/+}$) days after Stx2 injection. The *Adamts13B/CN1*$^{-/-}$ mouse developed symptoms as described (14) whereas the wild-type mouse did not. Further experiments were carried out with the C57BL/6-CAST/Ei mice treated with Stx2, *Adamts13*$^{-/-}$ n=6, *Adamts13*$^{+/-}$ n=3, *Adamts13*$^{+/+}$ n=3, or with PBS, *Adamts13*$^{-/-}$ n=4 and *Adamts13*$^{+/-}$ n=4 mice. Mice were sacrificed 48 hrs after Stx2 injection at which point no symptoms were noted, in all but one PBS-treated *Adamts13*$^{-/-}$ mouse that developed spontaneous TTP.

Immunofluorescence for detection of C3

Renal tissues (human and murine) were paraffin-embedded and sectioned as previously described (24). Sections were blocked with 5% bovine serum albumin (BSA, Sigma-Aldrich) in PBS (Medicago AB, Uppsala, Sweden) for 30 min. Human tissues were incubated with rabbit anti-human C3c (Dako, Glostrup, Denmark) at 19.2 μg/ml and mouse tissues were incubated with rabbit anti-mouse C3 (Hycult Biotech, Uden, The Netherlands) at 20 μg/ml, both in 2.5 % BSA in PBS for 1hr. Rabbit IgG (Dako) was used as the control antibody in both experiments at the same respective concentrations. Sections were washed twice with PBS for 5 min each. The signal was detected by incubating the slides with goat anti-rabbit (H+L) $F(ab)_2$ Alexa-Fluor 488 (Molecular Probes, Eugene, OR) at 1:150 dilution in 2.5 % BSA in PBS for 30 min followed by a washing step with shaking. The specificity of the secondary antibody was tested by omitting the primary antibody. Slides were mounted

with medium containing 4', 6-diamidino-2-phenylindole (DAPI, Vector Laboratories, Burlingame, CA) to stain the nuclei. Staining was visualized using a fluorescent microscope (Axiostar Zeiss, mounted with an AxioCam MRc5 camera, Carl Zeiss, Göttingen, Germany). For quantification of C3 labeling in mouse kidneys, 100 glomeruli/kidney were counted consecutively in the outer cortex starting from hilum. Slides were coded and blinded during this process.

Immunohistochemistry for detection of C5b-9

Immunohistochemistry was performed to detect C5b-9 in human renal tissues according to a described method (25) with some modifications. Briefly, after peroxidase blocking, antigen retrieval was achieved by incubating the tissues with 0.1% protease type X1V (Sigma) for 20 min at 37 °C followed by blocking with 5% BSA in tris-buffered saline (TBS, Medicago) for 2 hr at room temperature. C5b-9 was detected using mouse anti-human C5b-9 antibody (1:250, Dako) and mouse $IgG_2a\kappa$ (Dako) as the control antibody. The signal was detected using goat anti-mouse IgG:HRP (1:100, Dako). Positive signal stained brown and slides were examined by light microscope (Axiostar Zeiss mounted with an AxioCam MRc5 camera, Carl Zeiss, Göttingen, Germany).

Flow cytometry for detection of C3 and C9 on endothelial microparticles in plasma

Microparticles were isolated from plasma samples from patients 2-11 and controls (n=13) as described (7). Flow cytometry was performed using a FACSCanto II instrument with FACSDiva software version 6.0 (Becton Dickinson Immunocytometry Systems, San Jose, CA). Endothelial microparticle subpopulations were determined using mouse anti-human CD105: Percp Cy 5.5 (1:800, BD Biosciences, San Jose, CA) and mouse anti-human CD38:PE (1:100, BD Biosciences, to exclude monocyte-derived microparticles). Surface-bound C3 and C9 on these endothelial microparticles was detected using chicken anti-human C3:FITC (1:600, Diapensia, Linköping, Sweden) and mouse anti-human C9:FITC (1:100, Hycult Biotech), respectively. The C3 antibody recognizes all forms of C3 and the C9 antibody recognizes the neo-epitope of activated C9. Chicken anti-human insulin:FITC (1:800, Diapensia) or mouse IgG_1:FITC (Hycult Biotech) were used as the control antibodies.

Glomerular endothelial cells

Primary human glomerular microvascular endothelial cells (PGEC, Cell Systems, Kirkland WA) were grown in endothelial growth medium 2-microvascular (EGM-2MV) supplemented with growth factors, 5% fetal bovine serum (all from Lonza, Walkersville, MD) and 1x pencillin/streptomycin (PAA Laboratories). Cells were grown to confluence in T25 culture flasks (TPP, Trasadingen, Switzerland) at 37 °C with 5% CO_2 and used up to passage 10. Cells were detached from the culture flasks using 1x TrypLE (GIBCO, Grand Island, NY). The cells were then washed and resuspended in the same medium, without serum, and used in perfusion experiments.

Perfusion experiments for detection of platelet-endothelial interactions and complement deposition

Complement deposition on platelets and endothelial cells was studied using a semi-automated microfluidic platform (VenaFlux and Vena8 Endothelial+ biochips, Cellix, Dublin, Ireland) to mimic physiological flow conditions. Biochips were pre-coated with 12 μl of fibronectin/channel (100 μg/ml, Sigma-Aldrich) as an attachment factor. The PGEC suspension (10 μl) was added at 0.2×10^6 cells per channel and the biochip was incubated in the moist chamber at 37 °C with 5% CO_2 for 2 hr. To prevent drying after the initial 30

min of incubation, 40 μl of serum-free medium was added to the wells on each side of the channel.

The biochip was connected to a Mirus Evo nanopump (Cellix) allowing accurate shear stress. Unbound PGECs were washed away with DPBS at a shear stress of 20 dynes/cm^2 for 1 min. PGEC cells were stimulated with or without 200 μM histamine (Sigma-Aldrich) in DPBS at a shear stress of 5 dynes/cm^2 for 10 min. Histamine triggers VWF release from endothelial cells (26). To confirm VWF release from the cells, rabbit anti-human VWF (1:10, Dako) was perfused over the cells at 2.5 dynes/cm^2 for 5 min followed by swine anti-rabbit IgG: tetramethyl rhodamine isothiocyanate (TRITC 1:10) at the same shear stress.

Experiments with or without histamine stimulation were followed by perfusion with PRP or PPP/serum (with or without Ca^{+2} and Mg^{+2} supplementation) to which washed platelets at a concentration of 150-250 x 10^6 /ml (from one healthy donor/experiment) were added in certain experiments, at a shear stress of 5 dynes/cm^2 for 5 min. This shear stress corresponds to values in large veins and the descending aorta (27). In some experiments PGEC were first perfused with patient PPP combined with normal washed platelets followed by perfusion of normal plasma (as a source of ADAMTS13) or recombinant ADAMTS13 (rADAMTS13) (28) at a 1:25 dilution for an additional 5 min. To block the effect of ADAMTS13 (29) plasma/serum samples were pre-incubated with 20 mM ethylene diamine tetra-acetic acid (EDTA, Merck, Darmstadt, Germany) just before perfusion, in certain experiments. Plasma samples were likewise pre-incubated with 10mM ethylene glycol tetraacetic acid (EGTA, Complement Technology, Inc. Tyler, Texas) just before perfusion, in certain experiments. As a control, PGEC cells were exposed to perfused washed platelets without PPP/serum or PPP without platelets or heat-inactivated plasma under the same conditions.

To detect complement deposition on the cells, rabbit anti-human C3c:fluorescein isothiocyanate (FITC 1:25, Dako) or mouse anti-human C9:FITC (1:5) were perfused over the cells at 2.5 dynes/cm^2 for 5 min. The anti-C3c antibody recognizes all but C3a and C3dg. As a control antibody rabbit IgG:FITC (Abcam, Cambridge, UK) or mouse IgG1:FITC (Monosan, Uden, The Netherlands) was used. In some experiments VWF released from cells was stained with anti-VWF antibody followed by swine anti-rabbit IgG:TRITC antibody as above. Cells were then fixed with 0.5% paraformaldehyde and counter-stained for C3 deposition with the rabbit anti-human C3c:FITC antibody. Excess antibody was washed away with DPBS at the same shear stress. The fluorescent signal was visualized using a fluorescent microscope (Carl Zeiss Axiovert 40CFL, Jena, Germany) equipped with a digital camera DP 450 (Deltapix, Maalov, Denmark) to obtain real-time images. Pictures were analyzed using Image-Pro Plus software (Media Cybernetics, Bethesda, MD).

Flow cytometry for detection of C3 and C9 on endothelial microparticles released during platelet perfusion

In certain perfusion experiments plasma samples diluted 50% in DPBS supplemented with Ca^{+2} and Mg^{+2} were used. Normal washed platelets were added to the plasma and perfused onto histamine-stimulated glomerular endothelial cells as described above. The pre-sample was defined as the normal washed platelets added to plasma. Both the pre-samples and samples after perfusion were centrifuged twice at 2000 g for 10 min and 10000 g for 5 min and supernatants were collected. In these samples endothelial microparticle subpopulations were detected by flow cytometry as described above.

Statistical evaluation

Differences between ADAMTS13 wild-type and deficient mice treated with Stx or PBS with regard to C3 deposition in glomeruli, as well as differences between patients and controls regarding C3 and C9 deposition on endothelial microparticles in plasma and after perfusion, were analyzed by the Mann-Whitney U test. P values <0.05 were considered significant and the statistical analysis was performed by GraphPad Prism softare (GraphPad Software, Version 5, La Jolla, Ca).

Results

Complement deposition in human TTP kidneys

C3 deposition was demonstrated by immunofluorescence in and around glomerular endothelial capillaries and in tubuli in renal tissue from two TTP patients. Fig. 1*A* and 1*B* show the kidney of Patients 1 and 2 (Table I), respectively. Control renal tissue did not show any staining (Fig. 1*C*). The control antibody and omission of the primary antibody did not exhibit staining (data not shown).

Immunohistochemistry performed on renal tissues from the same patients exhibited C5b-9 deposition in few glomeruli and tubuli as well as on the intima of arterioli. Fig. 1*D* and 1*E* show renal tissue from Patient 1 and Patient 2, respectively. Control tissue was negative (Fig. 1*F*).

Renal complement deposition in a murine model of TTP

ADAMTS13-deficient mice were used to investigate if complement deposition occurred in a murine model of TTP. Treatment of ADAMTS13-deficient mice with Stx results in a syndrome closely resembling human TTP (14, 23). Renal tissue was obtained from Stx2-challenged *Adamts13*$^{-/-}$ (n=7), *Adamts13*$^{+/+}$ (n=4) or *Adamts13*$^{+/-}$ (n=3) mice demonstrating, by immunofluorescence, that *Adamts13*$^{-/-}$ mice (n=6 of 7) had considerable C3 deposition in glomeruli and tubuli (Fig. 2*A*-*B*) whereas wild-type or heterozygous mice did not (Fig. 2*C*-*D*). These results indicate that complement deposition was not primarily induced by Stx2. Kidneys from PBS-treated ADAMTS13-deficient (n=3 of 4 mice) and heterozygous mice (n=4) did not exhibit staining (Fig. 2*E* and 2*F*) in all but one mouse (data not shown). This PBS-treated mouse was symptomatic with evidence of spontaneous TTP based on the peripheral blood count. Thus complement deposition occurs in the TTP-model even in the absence of Stx-treatment.

Quantification of C3 labeling in the different groups of mice is presented in Fig. 2*G* and showed that Stx2-treated ADAMTS13-deficient mice had significantly more C3 labeling in glomeruli. C9 labeling was not carried out in mouse tissues. Taken together, these results demonstrate that murine TTP is also characterized by renal C3 deposition, which is dependent on ADAMTS13 deficiency.

Complement-coated endothelial microparticles in TTP plasma

In order to detect complement activation in TTP patients surface expression of complement C3 and C9 on endothelial microparticles was measured in plasma from TTP patients (n=9, Patients 3-11) and controls (n=13) (Table II) by flow cytometry. In comparison to controls, plasma from TTP patients exhibited significantly higher levels of endothelial microparticles with surface-bound C3 and C9.

ADAMTS13 deficiency leads to complement deposition on VWF-platelet strings and glomerular endothelial cells

A perfusion chamber was used to assay the formation of VWF-platelet strings with complement deposits under flow. VWF-platelet strings form on damaged endothelial cells and persist for a longer time in the setting of ADAMTS13 deficiency (30). Histamine-stimulated PGEC were exposed to PRP or PPP combined with normal washed platelets, from five patients (Patients 3-6 and 9 in Table I) or healthy donors (n=11) under perfusion. PGEC exhibited a rounded morphology after histamine stimulation to which VWF-platelet strings attached. Patient plasma contributed to the stable formation of multiple VWF-platelet strings on PGEC (Fig. 3*A*). rADAMTS13 (Fig. 3*B*) or normal plasma (data not shown) perfused over the VWF-platelet strings formed in patient plasma lead to clearing of strings within 0.5-5 min. In normal plasma fewer strings formed and were rapidly removed under flow (data not shown).

C3 deposition was detected on the VWF-platelet strings formed in plasma (PRP or PPP with normal washed platelets) from the five TTP patients (Fig. 3*C*). No C3 deposition was detected in these samples after exposure to rADAMTS13 (Fig. 3*D*) or normal plasma (data not shown). Similarly, no C3 was detected when normal plasma (PRP or PPP with normal washed platelets) was perfused over the PGEC (data not shown).

Plasma samples were preincubated with EDTA in order to block complement activation and ADAMTS13 cleavage activity and later perfused over PGEC as above. Patient samples exhibited long VWF-platelet strings, which lacked C3 labeling (data not shown). Normal plasma preincubated with EDTA also exhibited long VWF-platelet strings (Fig. 3*E*) without C3 deposition (Fig. 3*F*). Likewise, no C3 deposition on endothelial cells or strings was detected when heat-inactivated patient plasma was perfused over the cells (data not shown).

The specificity of the anti C3c-antibody was evaluated by perfusing normal washed platelets (without plasma) over the histamine-stimulated PGEC. Very long VWF-platelet strings were detected with no C3 staining (data not shown). No staining was detected when patient plasma samples (PRP or PPP with normal washed platelets) were labeled with the control antibody (data not shown).

In similarity, perfusion of serum from three patients (patients 3-5), combined with normal washed platelets, over histamine-stimulated PGEC resulted in the formation of VWF-platelet strings or platelet aggregates on the cells (Fig. 4*A*). The aggregates labeled positively for C3 (Fig. 4*B*). The rounded endothelial cells (Fig. 4*C*) to which aggregates attached exhibited positive C3 staining (Fig. 4*D*). Patient sera pre-incubated with EDTA did not exhibit complement labeling without the addition of Ca^{2+} and Mg^{2+}, but when these ions were added C3 deposition was observed even in the presence of EDTA (data not shown). Platelet aggregates were not observed when normal serum was perfused instead of patient serum (Fig. 4*E*) and hence no staining with the C3 antibody (Fig. 4*F*). Taken together, the results indicate that C3 deposition occurs on platelets and PGEC when ADAMTS13 is deficient. Using the same methodology C9 was not detected on VWF-platelet strings or endothelial cells.

Mechanisms by which complement activation occurs in ADAMTS13 deficiency

Complement activation via the alternative pathway—Patient or normal PPP with added platelets pre-incubated with EDTA and perfused over PGEC exhibited long VWF-platelet strings without C3 deposition as stated above (Fig. 3*E-F* and Table III). Perfusion of patient plasma (n=2, Patients 5 and 6) preincubated with EGTA did not abrogate C3

deposition and all strings were stained with the C3 antibody (Table III). This suggests that the alternative pathway plays a role in the observed complement activation.

The contribution of VWF from plasma versus PGEC to C3 deposition— Perfusion experiments were carried out with and without histamine stimulation as histamine induces the release of VWF from endothelial cells (26). Patient plasma (n=2, Patients 5 and 6) with added platelets exhibited multiple strings on histamine-stimulated PGEC. C3 deposition was detected on all strings. Endothelial cells that were not stimulated with histamine and perfused with the same patients' plasma (with washed platelets) exhibited fewer VWF-platelet strings and all these strings were stained for C3 (Table III). These results suggest that VWF-platelet strings mostly contained VWF from endothelial cells but that VWF from plasma made a partial contribution to formation of strings and that all strings bound C3.

C3 deposition PGEC and VWF in the absence of platelets—Perfusion of PPP from patients (n=3, Patients 4-6) on histamine-stimulated PGEC without added platelets led to C3 deposition. In order to determine if C3 deposited on VWF strings the samples were counterstained with antibody to VWF (Fig. 5*A*). The VWF strings were thus shown to bind C3 (Fig. 5*B* and 5*C*). The results indicate that C3 deposits directly on PGEC as well as on VWF strings and on activated platelets (Fig. 3*C*) binding to the VWF strings.

Release of C3- and C9-coated endothelial microparticles when plasma was perfused over PGEC

To mimic conditions in the vasculature endothelial cell-derived microparticles released during perfusion were assayed for C3 and C9 deposition. Using flow cytometry, surface expression of C3 and C9 on endothelial microparticles (defined as CD105-positive) released during perfusion experiments using plasma from TTP patients (n=6, Patients 3, 5, 6, 8, 9 and 12) and controls (n=6) was measured (Fig. 6). In comparison to controls, the pre-sample (patient plasma combined with normal platelets before perfusion over PGEC) from TTP patients showed more circulatory endothelial microparticles with surface-bound C9. Perfusion of plasma incubated with normal washed platelets over glomerular endothelial cells lead to the release of endothelial microparticles with surface-bound C3 and C9. This effect was significantly more pronounced in patients than controls (Fig. 6).

Discussion

The pathological hallmark of TTP is TMA characterized by thrombosis of small arteries, arterioles and capillaries with endothelial cell injury and platelet aggregation (31). Glomerular endothelial cells exhibit swelling and detachment from the basement membrane and platelet-VWF rich thrombi deposit in glomerular capillaries (32). Such an endothelial cell lesion would be enhanced by complement-associated injury. This study demonstrated that ADAMTS13 deficiency leads to C3 and C9 deposition in renal tissues from patients with TTP and to C3 deposition in the glomeruli of ADAMTS13-deficient mice. Endothelial microparticles in the TTP patient circulation were coated with C3 and C9. ADAMTS13 deficiency is known to mediate the adherence of platelets onto VWF strings released from endothelial cells (30). Here we demonstrated that TTP patient plasma/serum induced deposition of C3 on VWF-platelet strings deposited on glomerular endothelial cells as well as the release of C3 and C9-coated endothelial microparticles. Thus ADAMTS13 deficiency was shown to induce complement activation, which would be expected to induce and sustain endothelial and platelet activation within the TMA lesion.

Autopsies performed in the 1970s on two previously described TTP cases provided evidence for C3 deposition in patient tissues (33, 34). However, ADAMTS13 diagnostics was not available then and the possibility that these patients suffered from atypical HUS cannot be ruled out. A more recent case study demonstrated the presence of complement C3d, C4d and C5b-9 in the skin of a patient with acquired TTP (35). We demonstrated complement C3 and C5b-9 in the kidneys of two TTP patients with documented ADAMTS13 mutations thus showing that complement was activated in the kidney during TTP. Moreover, the finding of C3 in glomeruli of Stx2-treated *ADAMTS13*$^{-/-}$ mice implied that, in the setting of ADAMTS13 deficiency, complement was activated and deposited at the site of microvascular injury. As complement did not deposit in the Stx2-treated ADAMTS13-sufficient mice and did deposit in one symptomatic PBS-treated ADAMTS13-deficient mouse we conclude that ADAMTS13 deficiency, and not Stx2, promoted C3 deposition in these mice.

Previous studies have suggested that complement is activated during acute episodes of TTP with reduced levels of serum C3 or elevated platelet-bound C3 (16, 36-38), with the reservation that older studies did not apply ADAMTS13 diagnostics. A more recent study demonstrated high levels of C3a and sC5b-9 during the acute phase of TTP, normalizing at remission (15), although this study did not find a parallel decrease in serum C3. Furthermore, plasma from 8/49 patients with ADAMTS13 deficiency induced hemolysis of sheep erythrocytes (39). Indirectly, a role for complement activation was inferred when a case of TTP was successfully treated with the anti-human C5 antibody eculizumab (35). We demonstrate complement C3- and C9-coated endothelial microparticles in patient plasma during remission. This suggests that complement activation is ongoing in the microvascular process even in the absence of an overt recurrence of disease in patients with ADAMTS13 deficiency.

We show that when ADAMTS13 is deficient, complement is activated on VWF-platelet strings, glomerular endothelium and on microparticles derived from endothelial cells. It has been shown that complement deposition can occur on both activated platelets (13) and endothelial cells (9). Thus, when ADAMTS13 is deficient and larger platelet thrombi are allowed to form on damaged endothelium, complement deposition could occur on these cells. TTP sera allowed C3 and C5b-9 deposition to occur on microvascular endothelial cells and upregulated P selectin on the cells thus enhancing the cells capacity to bind neutrophils (16). TTP sera also increased neutrophil degranulation inducing a damaging effect on the cells (16), effects that were attributed to complement activation (40). In the current study we showed that C3 deposition on VWF strings is abolished by heat-inactivation of plasma as well as by addition of EDTA but not EGTA, the latter suggesting complement activation via the alternative pathway.

Shear-associated platelet adhesion to the endothelium and subendothelium occurs only in the presence of VWF (41). ULVWF multimers secreted by endothelial cells are more effective than large plasma VWF forms in supporting shear-induced aggregation (11). At lower shear, such as used in the current study, endothelial cells were shown to release VWF (42). Although this shear stress is lower than expected in glomerular capillaries it was chosen because higher shear was previously shown to reduce the formation of VWF-platelet strings (43) and also due to limitations in the volume of patient samples. ULVWF attach to the surface of histamine-stimulated endothelial cells and form large string-like structures to which platelets adhere. Shear induces tensile forces on ULVWF allowing exposure of the VWF cleavage site on the A2 domain and thus cleavage of VWF-platelet strings by ADAMTS13 (30).

In the current study there was no C3 deposition on the VWF-platelet strings formed by perfusion of washed platelets alone (without plasma) over PGEC. As all strings bound C3 regardless of histamine stimulation, and as plasma contains a considerably higher concentration of C3 than cell supernatants we presume that the C3 bound to VWF-platelet strings originated from plasma. On the other hand, most of the VWF to which C3 bound originated from the endothelial cells and a smaller fraction from the perfused plasma. Interestingly, we could demonstrate that C3 deposited on platelets that were bound to VWF strings and also on the VWF strings themselves. This is in line with a recent publication showing C3 bound to VWF strings on human umbilical vein endothelial cells under static conditions (44).

Histamine stimulation induced an increase in the number of VWF-platelet strings and thus more C3 deposition (Table III). Complement by-products C3a and C5a have been shown to be involved in the release of histamine from mast cells (45). Hence, in patient circulation, complement activation with subsequent release of C3a and C5a could induce the release of histamine, which would be involved in further release of ULVWF from endothelial cells followed by more complement deposition. Patient and control samples were collected in citrated or serum tubes. Sodium citrate is used an anti-coagulant which may also partially inactivate the complement system by chelating calcium. Serum is collected after clot formation, during which a certain degree of complement activation occurs ex vivo. Plasma samples were not available in hirudin, or lepirudin, both of which bind thrombin without affecting the complement cascade (46), and would thereby allow a more accurate assessment of complement activation in vitro. Thus the results may represent an underestimation of the degree of complement activation that could potentially occur.

An interesting finding was the presence of C3 and C9 on circulatory endothelial microparticles. Endothelial microparticles have been previously described in various inflammatory and thrombotic diseases (47) including TTP (48). They have procoagulant potential, carry VWF (49) and form aggregates with platelets in the presence of ristocetin (50). Endothelial microparticles originating from brain or renal endothelium may contain more VWF and thus possess higher aggregative potential (50). In addition to their thrombogenic potential, endothelial microparticles from TTP patients were recently found to generate fibrinolytic activity (51). The deposition of complement on endothelial microparticles may indicate that complement deposited on the parent cells during cellular injury before microvesicle membrane budding occurred, or that complement deposited on the microparticles themselves. Complement deposition directly on microparticles could occur for the purpose of opsonization and disposal. The presence of C5b-9 on the endothelial membrane can increase the procoagulant potential of endothelial cells (52) and most probably of endothelial cell-derived microparticles.

Complement activation mediates the thrombotic lesion occurring in atypical HUS due to complement mutations and dysfunction (53). The pathological lesion is very similar to TMA in TTP. In TTP complement activation is most probably a secondary phenomenon occurring in response to platelet activation on damaged endothelium. Regardless of the cause complement activation will contribute to the thrombotic process, through enhanced platelet activation (13) and endothelial damage, and thus sustain the microangiopathic lesion.

Acknowledgments

We are grateful to the physicians caring for the TTP patients not in our direct care who provided blood samples and/or clinical information, including Drs Peter Björk, Virginia Strineholm, Ulf Tedgård, Rolf Billström, Ingemar Winqvist, Göran Oldaeus, Johan Richter, Per Dahlberg and to the patients who participated in this study.

Financial support:

This study was supported by grants from The Swedish Research Council (K2013-64X-14008), The Torsten Söderberg Foundation, Crown Princess Lovisa's Society for Child Care, The Konung Gustaf V:s 80-årsfond, (all to DK) and by NIH/NHLBI 1R0HL106495-01 to DM. A preliminary version of this paper appeared in the Ph.D. thesis of Dr. Ramesh Tati.

References

1. Ruggenenti P, Noris M, Remuzzi G. Thrombotic microangiopathy, hemolytic uremic syndrome, and thrombotic thrombocytopenic purpura. Kidney Int. 2001; 60:831–846. [PubMed: 11532079]
2. Furlan M, Robles R, Solenthaler M, Wassmer M, Sandoz P, Lammle B. Deficient activity of von Willebrand factor-cleaving protease in chronic relapsing thrombotic thrombocytopenic purpura. Blood. 1997; 89:3097–3103. [PubMed: 9129011]
3. Levy GG, Nichols WC, Lian EC, Foroud T, McClintick JN, McGee BM, Yang AY, Siemieniak DR, Stark KR, Gruppo R, Sarode R, Shurin SB, Chandrasekaran V, Stabler SP, Sabio H, Bouhassira EE, Upshaw JD Jr. Ginsburg D, Tsai HM. Mutations in a member of the ADAMTS gene family cause thrombotic thrombocytopenic purpura. Nature. 2001; 413:488–494. [PubMed: 11586351]
4. Tsai HM, Lian EC. Antibodies to von Willebrand factor-cleaving protease in acute thrombotic thrombocytopenic purpura. N Engl J Med. 1998; 339:1585–1594. [PubMed: 9828246]
5. Besbas N, Karpman D, Landau D, Loirat C, Proesmans W, Remuzzi G, Rizzoni G, Taylor CM, Van de Kar N, Zimmerhackl LB. A classification of hemolytic uremic syndrome and thrombotic thrombocytopenic purpura and related disorders. Kidney Int. 2006; 70:423–431. [PubMed: 16775594]
6. Ståhl AL, Sartz L, Nelsson A, Bekassy ZD, Karpman D. Shiga toxin and lipopolysaccharide induce platelet-leukocyte aggregates and tissue factor release, a thrombotic mechanism in hemolytic uremic syndrome. PLoS One. 2009; 4:e6990. [PubMed: 19750223]
7. Ståhl AL, Sartz L, Karpman D. Complement activation on platelet-leukocyte complexes and microparticles in enterohemorrhagic Escherichia coli-induced hemolytic uremic syndrome. Blood. 2011; 117:5503–5513. [PubMed: 21447825]
8. Louise CB, Obrig TG. Shiga toxin-associated hemolytic uremic syndrome: combined cytotoxic effects of shiga toxin and lipopolysaccharide (endotoxin) on human vascular endothelial cells in vitro. Infect Immun. 1992; 60:1536–1543. [PubMed: 1548077]
9. Morigi M, Galbusera M, Gastoldi S, Locatelli M, Buelli S, Pezzotta A, Pagani C, Noris M, Gobbi M, Stravalaci M, Rottoli D, Tedesco F, Remuzzi G, Zoja C. Alternative pathway activation of complement by Shiga toxin promotes exuberant C3a formation that triggers microvascular thrombosis. J Immunol. 2011; 187:172–180. [PubMed: 21642543]
10. Manuelian T, Hellwage J, Meri S, Caprioli J, Noris M, Heinen S, Jozsi M, Neumann HP, Remuzzi G, Zipfel PF. Mutations in factor H reduce binding affinity to C3b and heparin and surface attachment to endothelial cells in hemolytic uremic syndrome. J Clin Invest. 2003; 111:1181–1190. [PubMed: 12697737]
11. Moake JL, Turner NA, Stathopoulos NA, Nolasco LH, Hellums JD. Involvement of large plasma von Willebrand factor (vWF) multimers and unusually large vWF forms derived from endothelial cells in shear stress-induced platelet aggregation. J Clin Invest. 1986; 78:1456–1461. [PubMed: 3491092]
12. Vaziri-Sani F, Holmberg L, Sjöholm AG, Kristoffersson AC, Manea M, Fremeaux-Bacchi V, Fehrman-Ekholm I, Raafat R, Karpman D. Phenotypic expression of factor H mutations in patients with atypical hemolytic uremic syndrome. Kidney Int. 2006; 69:981–988. [PubMed: 16528247]
13. Ståhl AL, Vaziri-Sani F, Heinen S, Kristoffersson AC, Gydell KH, Raafat R, Gutierrez A, Beringer O, Zipfel PF, Karpman D. Factor H dysfunction in patients with atypical hemolytic uremic syndrome contributes to complement deposition on platelets and their activation. Blood. 2008; 111:5307–5315. [PubMed: 18268093]
14. Motto DG, Chauhan AK, Zhu G, Homeister J, Lamb CB, Desch KC, Zhang W, Tsai HM, Wagner DD, Ginsburg D. Shigatoxin triggers thrombotic thrombocytopenic purpura in genetically susceptible ADAMTS13-deficient mice. J Clin Invest. 2005; 115:2752–2761. [PubMed: 16200209]

15. Reti M, Farkas P, Csuka D, Razso K, Schlammadinger A, Udvardy ML, Madach K, Domjan G, Bereczki C, Reusz GS, Szabo AJ, Prohaszka Z. Complement activation in thrombotic thrombocytopenic purpura. J Thromb Haemost. 2012; 10:791–798. [PubMed: 22372946]
16. Ruiz-Torres MP, Casiraghi F, Galbusera M, Macconi D, Gastoldi S, Todeschini M, Porrati F, Belotti D, Pogliani EM, Noris M, Remuzzi G. Complement activation: the missing link between ADAMTS-13 deficiency and microvascular thrombosis of thrombotic microangiopathies. Thromb Haemost. 2005; 93:443–452. [PubMed: 15735793]
17. Assink K, Schiphorst R, Allford S, Karpman D, Etzioni A, Brichard B, van de Kar N, Monnens L, van den Heuvel L. Mutation analysis and clinical implications of von Willebrand factor-cleaving protease deficiency. Kidney Int. 2003; 63:1995–1999. [PubMed: 12753286]
18. Karpman D, Holmberg L, Jirgard L, Lethagen S. Increased platelet retention in familial recurrent thrombotic thrombocytopenic purpura. Kidney Int. 1996; 49:190–199. [PubMed: 8770967]
19. Manea M, Kristoffersson A, Tsai HM, Zhou W, Winqvist I, Oldaeus G, Billstrom R, Björk P, Holmberg L, Karpman D. ADAMTS13 phenotype in plasma from normal individuals and patients with thrombotic thrombocytopenic purpura. Eur J Pediatr. 2007; 166:249–257. [PubMed: 17187257]
20. Schneppenheim R, Kremer Hovinga JA, Becker T, Budde U, Karpman D, Brockhaus W, Hrachovinova I, Korczowski B, Oyen F, Rittich S, von Rosen J, Tjonnfjord GE, Pimanda JE, Wienker TF, Lammle B. A common origin of the 4143insA ADAMTS13 mutation. Thromb Haemost. 2006; 96:3–6. [PubMed: 16807643]
21. Richter J, Strandberg K, Lindblom A, Strevens H, Karpman D, Wide-Swensson D. Successful management of a planned pregnancy in severe congenital thrombotic thrombocytopaenic purpura: the Upshaw-Schulman syndrome. Transfus Med. 2011; 21:211–213. [PubMed: 21219489]
22. Manea M, Kristoffersson A, Schneppenheim R, Saleem MA, Mathieson PW, Mörgelin M, Björk P, Holmberg L, Karpman D. Podocytes express ADAMTS13 in normal renal cortex and in patients with thrombotic thrombocytopenic purpura. Br J Haematol. 2007; 138:651–662. [PubMed: 17627784]
23. Huang J, Motto DG, Bundle DR, Sadler JE. Shiga toxin B subunits induce VWF secretion by human endothelial cells and thrombotic microangiopathy in ADAMTS13-deficient mice. Blood. 2010; 116:3653–3659. [PubMed: 20644116]
24. Shi SR, Key ME, Kalra KL. Antigen retrieval in formalin-fixed, paraffin-embedded tissues: an enhancement method for immunohistochemical staining based on microwave oven heating of tissue sections. J Histochem Cytochem. 1991; 39:741–748. [PubMed: 1709656]
25. Schmitt R, Carlsson F, Mörgelin M, Tati R, Lindahl G, Karpman D. Tissue deposits of IgA-binding streptococcal M proteins in IgA nephropathy and Henoch-Schonlein purpura. Am J Pathol. 2010; 176:608–618. [PubMed: 20056836]
26. Nolasco LH, Turner NA, Bernardo A, Tao Z, Cleary TG, Dong JF, Moake JL. Hemolytic uremic syndrome-associated Shiga toxins promote endothelial-cell secretion and impair ADAMTS13 cleavage of unusually large von Willebrand factor multimers. Blood. 2005; 106:4199–4209. [PubMed: 16131569]
27. Papaioannou TG, Stefanadis C. Vascular wall shear stress: basic principles and methods. Hellenic J Cardiol. 2005; 46:9–15. [PubMed: 15807389]
28. Manea M, Tati R, Karlsson J, Bekassy ZD, Karpman D. Biologically active ADAMTS13 is expressed in renal tubular epithelial cells. Pediatr Nephrol. 2010; 25:87–96. [PubMed: 19644711]
29. Tati R, Kristoffersson AC, Ståhl AL, Mörgelin M, Motto D, Satchell S, Mathieson P, Manea-Hedstrom M, Karpman D. Phenotypic expression of ADAMTS13 in glomerular endothelial cells. PLoS One. 2011; 6:e21587. [PubMed: 21720563]
30. Lopez JA, Dong JF. Cleavage of von Willebrand factor by ADAMTS-13 on endothelial cells. Semin Hematol. 2004; 41:15–23. [PubMed: 14727255]
31. Benz K, Amann K. Pathological aspects of membranoproliferative glomerulonephritis (MPGN) and haemolytic uraemic syndrome (HUS) / thrombocytic thrombopenic purpura (TTP). Thromb Haemost. 2009; 101:265–270. [PubMed: 19190808]
32. Manea M, Karpman D. Molecular basis of ADAMTS13 dysfunction in thrombotic thrombocytopenic purpura. Pediatr Nephrol. 2009; 24:447–458. [PubMed: 18807073]

33. Mant MJ, Cauchi MN, Medley G. Thrombotic thrombocytopenic purpura: report of a case with possible immune etiology. Blood. 1972; 40:416–421. [PubMed: 4626870]
34. Weisenburger DD, O'Conner ML, Hart MN. Thrombotic thrombocytopenic purpura with C'3 vascular deposits: report of a case. Am J Clin Pathol. 1977; 67:61–63. [PubMed: 556662]
35. Chapin J, Weksler B, Magro C, Laurence J. Eculizumab in the treatment of refractory idiopathic thrombotic thrombocytopenic purpura. Br J Haematol. 2012; 157:772–774. [PubMed: 22409250]
36. Garvey MB, Freedman J. Complement in thrombotic thrombocytopenic purpura. Am J Hematol. 1983; 15:397–398. [PubMed: 6685975]
37. Noris M, Ruggenenti P, Perna A, Orisio S, Caprioli J, Skerka C, Vasile B, Zipfel PF, Remuzzi G. Hypocomplementemia discloses genetic predisposition to hemolytic uremic syndrome and thrombotic thrombocytopenic purpura: role of factor H abnormalities. Italian Registry of Familial and Recurrent Hemolytic Uremic Syndrome/Thrombotic Thrombocytopenic Purpura. J Am Soc Nephrol. 1999; 10:281–293. [PubMed: 10215327]
38. Wright JF, Wang H, Hornstein A, Hogarth M, Mody M, Garvey MB, Blanchette V, Rock G, Freedman J. Characterization of platelet glycoproteins and platelet/endothelial cell antibodies in patients with thrombotic thrombocytopenic purpura. Br J Haematol. 1999; 107:546–555. [PubMed: 10583256]
39. Feng S, Kroll MH, Nolasco L, Moake J, Afshar-Kharghan V. Complement activation in thrombotic microangiopathies. Br J Haematol. 2013; 160:404–406. [PubMed: 23116127]
40. Noris M, Mescia F, Remuzzi G. STEC-HUS, atypical HUS and TTP are all diseases of complement activation. Nat Rev Nephrol. 2012; 8:622–633. [PubMed: 22986360]
41. Savage B, Saldivar E, Ruggeri ZM. Initiation of platelet adhesion by arrest onto fibrinogen or translocation on von Willebrand factor. Cell. 1996; 84:289–297. [PubMed: 8565074]
42. Galbusera M, Zoja C, Donadelli R, Paris S, Morigi M, Benigni A, Figliuzzi M, Remuzzi G, Remuzzi A. Fluid shear stress modulates von Willebrand factor release from human vascular endothelium. Blood. 1997; 90:1558–1564. [PubMed: 9269774]
43. Dong JF, Moake JL, Nolasco L, Bernardo A, Arceneaux W, Shrimpton CN, Schade AJ, McIntire LV, Fujikawa K, Lopez JA. ADAMTS-13 rapidly cleaves newly secreted ultralarge von Willebrand factor multimers on the endothelial surface under flowing conditions. Blood. 2002; 100:4033–4039. [PubMed: 12393397]
44. Turner NA, Moake J. Assembly and activation of alternative complement components on endothelial cell-anchored ultra-large von Willebrand factor links complement and hemostasis-thrombosis. PLoS One. 2013; 8:e59372. [PubMed: 23555663]
45. el-Lati SG, Dahinden CA, Church MK. Complement peptides C3aand C5a-induced mediator release from dissociated human skin mast cells. J Invest Dermatol. 1994; 102:803–806. [PubMed: 7513741]
46. Bexborn F, Engberg AE, Sandholm K, Mollnes TE, Hong J, Nilsson Ekdahl K. Hirudin versus heparin for use in whole blood in vitro biocompatibility models. J Biomed Mater Res A. 2009; 89:951–959. [PubMed: 18470919]
47. Chironi GN, Boulanger CM, Simon A, Dignat-George F, Freyssinet JM, Tedgui A. Endothelial microparticles in diseases. Cell Tissue Res. 2009; 335:143–151. [PubMed: 18989704]
48. Jimenez JJ, Jy W, Mauro LM, Horstman LL, Ahn YS. Elevated endothelial microparticles in thrombotic thrombocytopenic purpura: findings from brain and renal microvascular cell culture and patients with active disease. Br J Haematol. 2001; 112:81–90. [PubMed: 11167788]
49. Jimenez JJ, Jy W, Mauro LM, Horstman LL, Soderland C, Ahn YS. Endothelial microparticles released in thrombotic thrombocytopenic purpura express von Willebrand factor and markers of endothelial activation. Br J Haematol. 2003; 123:896–902. [PubMed: 14632781]
50. Jy W, Jimenez JJ, Mauro LM, Horstman LL, Cheng P, Ahn ER, Bidot CJ, Ahn YS. Endothelial microparticles induce formation of platelet aggregates via a von Willebrand factor/ristocetin dependent pathway, rendering them resistant to dissociation. J Thromb Haemost. 2005; 3:1301–1308. [PubMed: 15946221]
51. Lacroix R, Plawinski L, Robert S, Doeuvre L, Sabatier F, Martinez de Lizarrondo S, Mezzapesa A, Anfosso F, Leroyer A, Poullin P, Jourde N, Njock MS, Boulanger C, Angles-Cano E, Dignat-

George F. Leukocyte- and endothelial-derived microparticles: a circulating source for fibrinolysis. Haematologica. 2012

52. Tedesco F, Pausa M, Nardon E, Introna M, Mantovani A, Dobrina A. The cytolytically inactive terminal complement complex activates endothelial cells to express adhesion molecules and tissue factor procoagulant activity. J Exp Med. 1997; 185:1619–1627. [PubMed: 9151899]
53. Loirat C, Noris M, Fremeaux-Bacchi V. Complement and the atypical hemolytic uremic syndrome in children. Pediatr Nephrol. 2008; 23:1957–1972. [PubMed: 18594873]

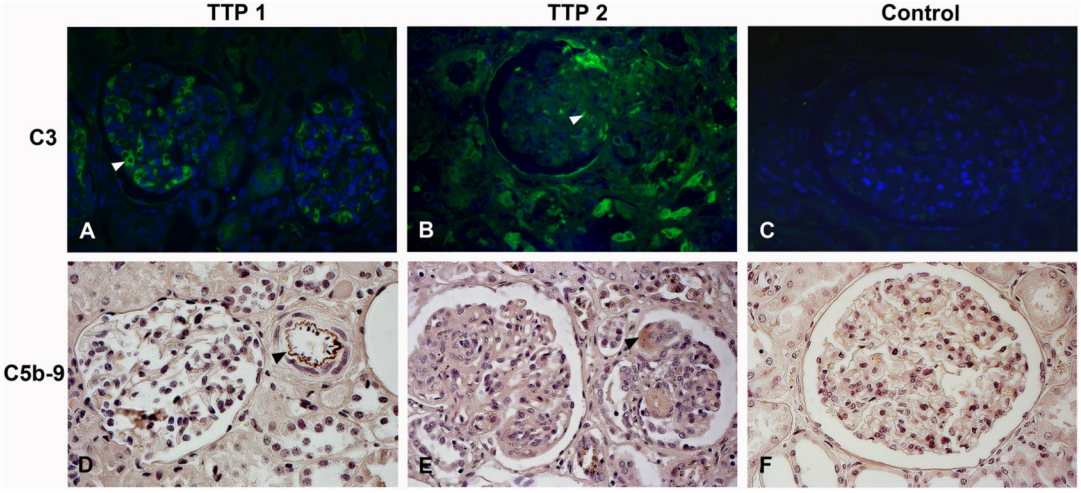

FIGURE 1. Complement deposition in human kidney from TTP patients

C3 deposition on human renal tissues was studied by immunofluorescence. Renal tissue from Patient 1 (A) and Patient 2 (B) showed C3 deposition in and around glomerular endothelial capillaries (see arrowhead in A) and in thrombi (see arrowhead in B). (C) Control human tissue exhibited no staining. C5b-9 deposition in human renal tissues was studied by immunohistochemistry exhibiting labeling in the intima of a cortical arteriolus (D, see arrow, Patient 1) and in a glomerular thrombus (E, see arrow, Patient 2). Labeling could not be demonstrated in control tissue (F). All images were taken at 400 x magnification.

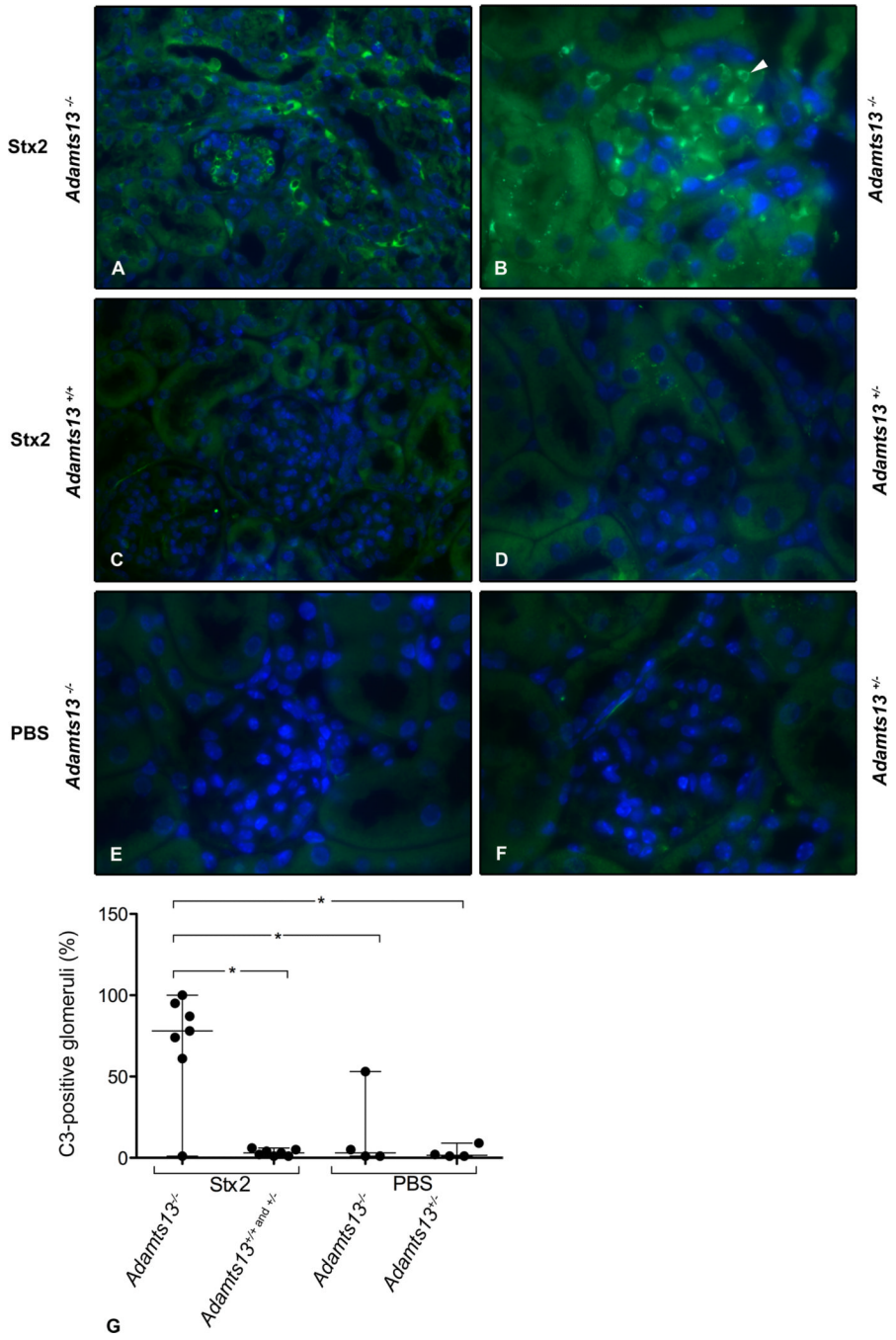

FIGURE 2. C3 deposition in Stx2-treated *Adamts13*$^{-/-}$ mice

C3 staining was observed in glomeruli and tubuli in the Stx2-treated *Adamts13B/CN1*$^{-/-}$ mouse with the mixed B/129-CASA/Rk genetic background (A) and *Adamts13*$^{-/-}$ mice with the CAST/Ei genetic background (B). Tissues from Stx2-treated *Adamts13B/CN1*$^{+/+}$ mouse (C) and *Adamts13*$^{+/-}$ mice (D) did not label for C3. PBS-treated *Adamts13*$^{-/-}$ (E) and *Adamts13*$^{+/-}$ (F) mice did not show any staining in the glomeruli. Images were taken at 400 x (A and C) and 1000 x (C-F) magnification. Quantification of C3-positive glomeruli in mice with both genetic backgrounds (mixed B/129-CASA/Rk and mixed C57BL/6-CAST/Ei) are presented (G). Stx2-treated *Adamts13*$^{-/-}$ mice (n=6 of 7) showed significantly more C3-stained glomeruli in comparison to wild-type *Adamts13*$^{+/+}$ (n=4) or heterozygous mice

Adamts13$^{+/-}$ (n=3) and PBC-treated mice (*Adamts13*$^{-/-}$ n=3 of 4 and *Adamts13*$^{+/-}$ n=4). Data are presented as median (horizontal bar) and range. *P <0.05.

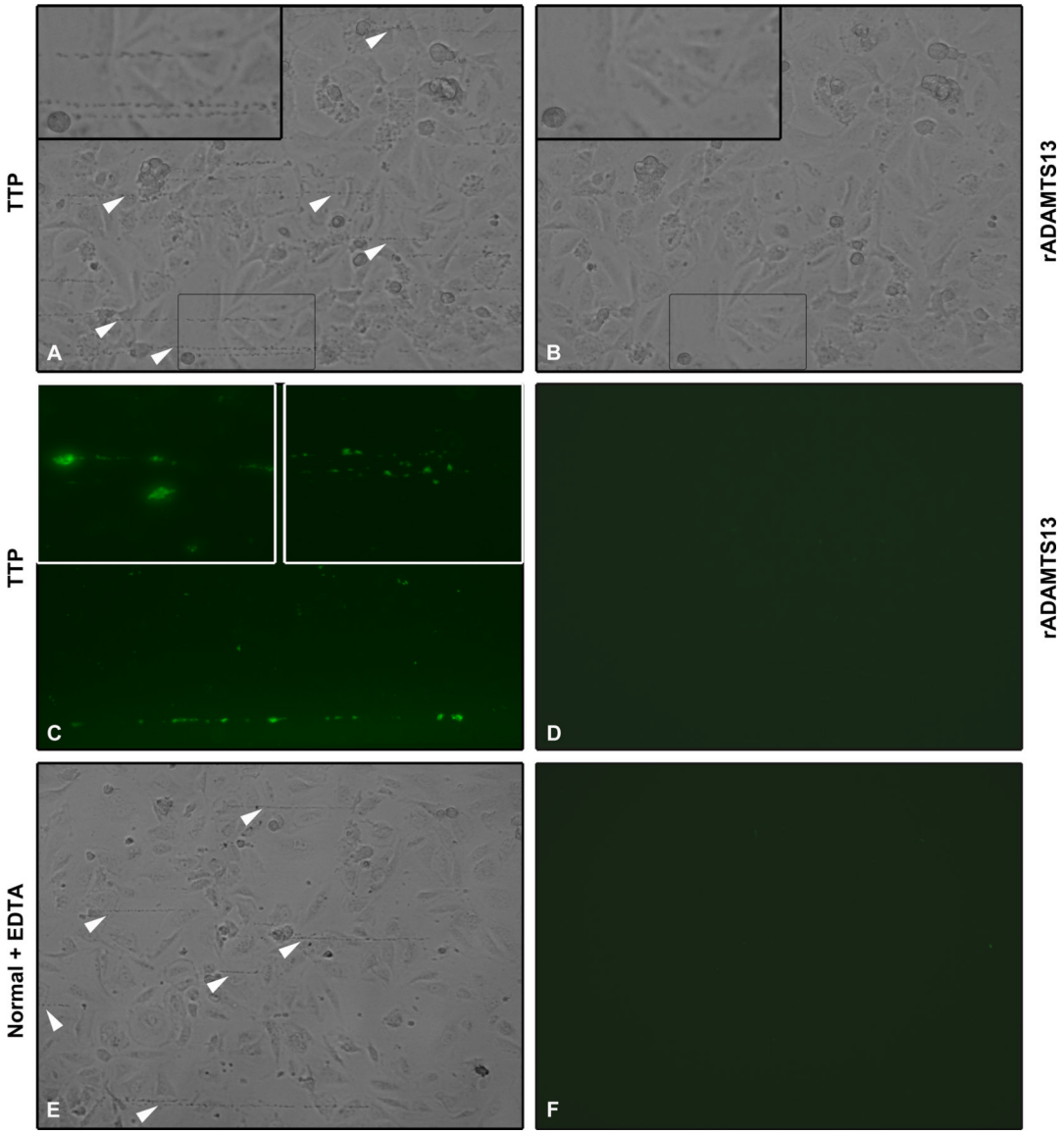

FIGURE 3. ADAMTS13 deficiency leads to VWF-platelet string formation and C3 deposition under flow

Histamine-pretreated PGEC cells were perfused with PRP. (A) Perfusion of PRP from TTP Patient 4 led to formation of VWF-platelet strings (arrowheads). The inset shows the VWF-platelet strings at a higher magnification. (B) rADAMTS13 was perfused over these strings (at the same location) at the same shear, clearing the strings within 3 mins. The inset at higher magnification demonstrates lack of strings. (C) VWF-platelet strings from TTP patients stained positively for C3 as shown here in a sample from Patient 3. Insets show C3 staining on the VWF-platelet strings from Patient 3 (left, higher magnification) and Patient 2 (right). (D) No C3 staining was visible on cells exposed to rADAMTS13 under flow. (E) Cells perfused with normal PRP pre-incubated with EDTA which inhibited the cleavage of VWF-platelet strings (arrowheads). (F) The strings shown in panel E did not stain for C3. Images are representative of six different experiments with reproducible results from five patients. Images were taken at 200x magnification (A-F and right inset in panel C), the left inset in panel C was taken at 400x magnification.

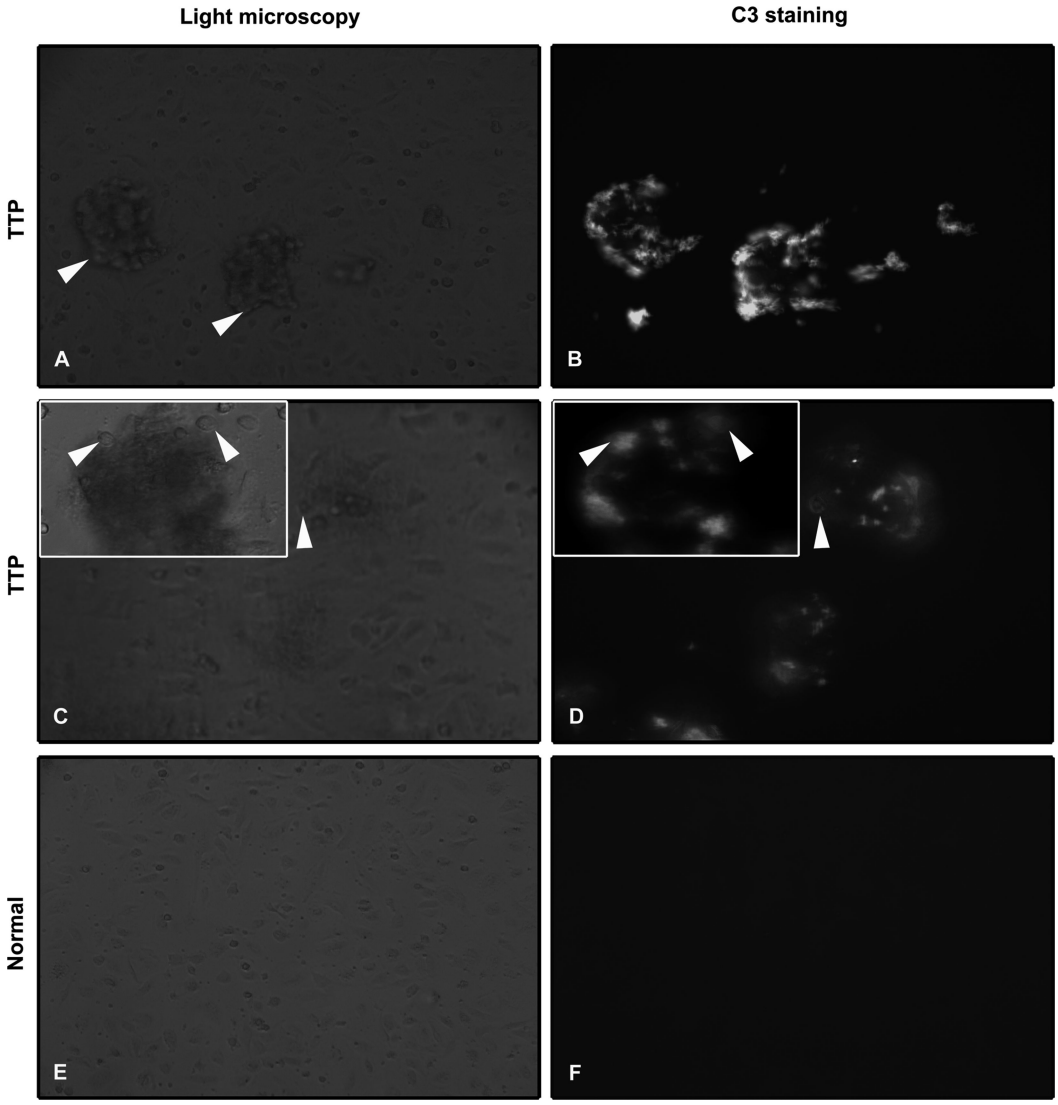

FIGURE 4. ADAMTS13 deficiency leads to platelet aggregation and C3 deposition on glomerular endothelial cells under flow

Histamine-pretreated PGEC cells were perfused with serum and normal washed platelets. (A) Perfusion of serum from TTP Patient 4 together with normal washed platelets led to platelet aggregation on the endothelial cells (arrowheads). (B) The aggregates shown in panel A stained positively for C3. (C) Endothelial cells that lodge the platelet aggregates differed morphologically and were rounder in shape (arrowhead). The inset shows similar morphological changes from a different region. (D) The cells shown in panel C stained positively for C3 (arrowheads). (E) Perfusion of normal serum with normal washed platelets did not result in formation of platelet aggregates and no C3 staining was visible (F). Images were taken at 200x magnification (A-F), both the insets in panel C and D were taken at 400x magnification. Reproducible results were obtained from three patients.

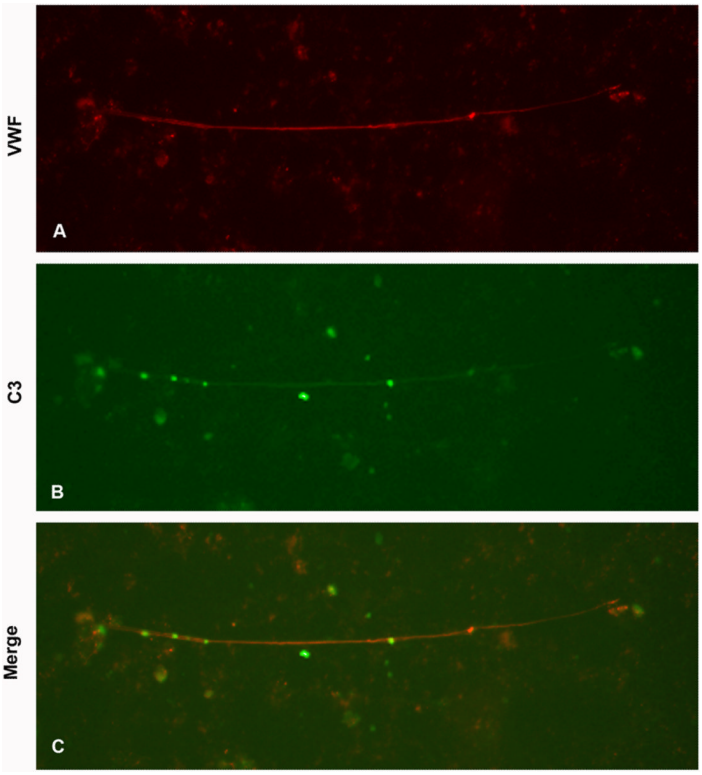

FIGURE 5. Complement deposition on VWF

Histamine-pretreated PGEC cells were perfused with plasma (but no platelets) and labeled with anti-human VWF and anti-human C3c. (A) Perfusion of PPP from TTP Patient 5, exhibited VWF strings stained for VWF. (B) The same VWF string was counter-stained for C3c. (C) Merged image showing staining for both VWF and C3. Images are representative of three different experiments with reproducible results from three patients. Images were taken at 200x magnification.

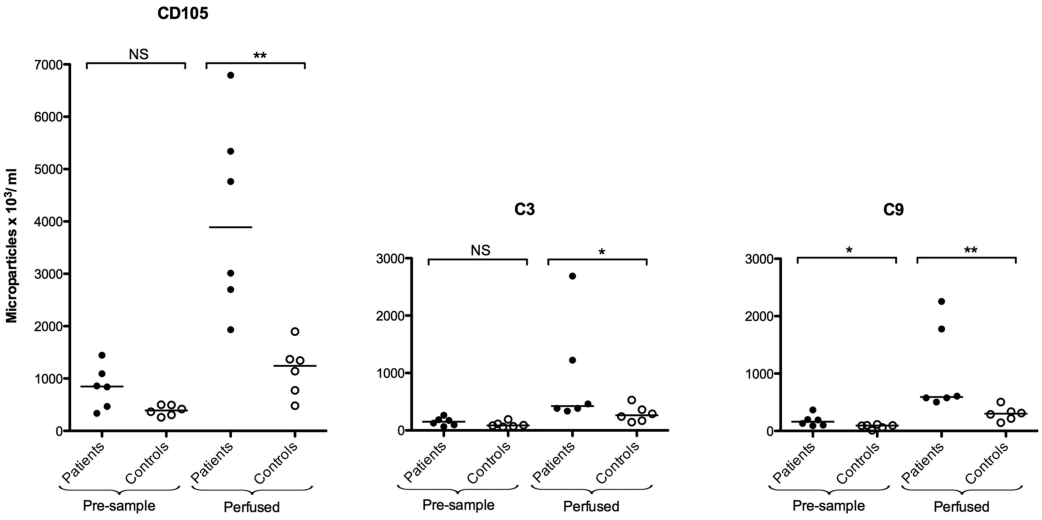

FIGURE 6. Complement deposition on endothelial microparticles released under perfusion

Plasma samples from TTP patients (n= 6) 3, 5, 6, 8, 9 and 12 (●) and controls (○, n=6) were perfused over histamine-stimulated glomerular endothelial cells and complement deposited on released endothelial-derived microparticles. Pre-perfusion plasma samples exposed to normal washed platelets showed more C3 and C9-coated endothelial microparticles in patient plasma than in controls. After perfusion patient samples induced more release of endothelial microparticles (CD105-positive, left), with C3 (middle) and C9 deposits (right). NS: not significant, $*P<0.05$.

Table I

Description of TTP patients included in this study

Patient number	Sex	Current age	Number of TTP episodes	ADAMTS13 mutation / polymorphism/auto-antibodies	Sample	At the time of sampling		References
						Age (yrs)	Treatment	
1	F	29	> 5	P353L, P457L	Renal biopsy[a]	2	FFP	(17)
2	F	-	-	4143insA[b]	Renal tissue	3.5	-	(22)
3	M	26	> 5	4143insA homozygous[c]	PRP, PPP, serum[d]	26	FFP	(17-20)
4	M	24	> 5	4143insA homozygous[c]	PRP, PPP, serum[d]	24	FFP	(17-20)
5	F	38	2	R1060W heterozygous R7W, A900V, A1033T	PRP, PPP, serum[d]	38	Low-dose acetyl salicylic acid	(21)
6	F	26	> 5	4143insA, P457L	PPP[d]	22	FFP	-
7	M	7	> 5	4143insA heterozygous[e]	PPP[d]	2	FFP	-
8	M	45	> 5	4143insA homozygous	PPP[d]	39	FFP	(19)
9	M	15	4	P671L, 4143insA	PRP, PPP[d]	7	FFP, insulin	(19)
10	F	50	2	Auto-antibodies	PPP[d]	42	FFP	(19)
11	F	81	> 5	Auto-antibodies	PPP[d]	70	FFP	(19)
12	F	39	1	Auto-antibodies[f]	PPP[d]	39	FFP, prednisolone	-

FFP: fresh frozen plasma, PRP: platelet-rich-plasma, PPP: platelet-poor-plasma.

[a] An open wedge biopsy was performed in in 1985 during the fourth episode of TTP in order to determine the diagnosis with certainty.

[b] Genetic work-up was not carried out on this patient who died at the age of 3.5 years in 1968 and renal tissue was obtained at autopsy. Her younger brother was later diagnosed with TTP (Patient 8) and a homozygous mutation was found. The unaffected parents bear the heterozygous mutation.

[c] Patients 3 and 4 are brothers.

[d] In these patients blood samples were obtained just before plasma infusion.

[e] The 4143insA mutation was inherited from the patient's mother. A mutation on the other allele was not investigated.

[f] Diagnostic work-up has not been completed in this patient in which ADAMTS13 activity was undetectable and a low level of auto-antibodies was found.

Table II

Complement deposition on endothelial microparticles in plasma from TTP patients and controls

Endothelial microparticles (× 10^3/ml)	TTP patients (n=9)	Controls (n=13)	*P* value
CD105	1104 (927-2433)	8.8 (1-410)	<0.0001
C3[a]	516 (318-978)	1.2 (1-68)	<0.0001
C9[a]	372 (168-1158)	1.2 (1-82)	<0.0001

Data are expressed as median and range of microparticles positive for each marker.

[a]Complement deposition on CD105-positive microparticles.

Table III

Complement deposition on VWF strings exposed to TTP patient plasma

Treatment	TTP	
	VWF strings[a]	% C3 positive
Histamine/PRP	20-25	100%
DPBS/PRP	10-12	100%
Histamine/PRP/EDTA	20-30	0%
Histamine/PRP/EGTA	10-12	100%
Histamine/PPP	20-30	100%

PRP: platelet-rich-plasma, PPP: platelet-poor-plasma.

Data represent results from 2-3 experiments.

[a]VWF strings (in the entire channel) with and without attached platelets.